# High-surface-area and nitrogen-rich mesoporous carbon material from fishery waste for effective adsorption of methylene blue

CrossMark

F. Marrakchi [a], M. Auta [b], W.A. Khanday [a,c], B.H. Hameed [a,*]

[a] School of Chemical Engineering, Engineering Campus, Universiti Sains Malaysia, 14300 Nibong Tebal, Penang, Malaysia
[b] Department of Chemical Engineering, Federal University of Technology, Minna, Nigeria
[c] Department of Chemistry, Govt. Degree College, Anantnag 192102, Jammu & Kashmir, India

## ARTICLE INFO

## ABSTRACT

A high quality nitrogen-rich mesoporous carbon material (FSAC) was prepared from carbonized fishery waste through chemical activation using NaOH. The obtained material had a high surface area of 1867 $m^2/g$, pore size of 2.5 nm and mesopore volume of 0.38 $cm^3/g$. The adsorption efficiency of FSAC was examined for methylene blue (MB) removal from aqueous solution in batch method. The effects of initial concentration of dye (25–400 mg/L), temperature (30–50 °C) and pH (3 − 11) on the adsorption of MB on FSAC were studied. Evaluation of MB uptake by FSAC revealed that Langmuir isotherm and pseudo-second-order adsorption model adequately described the experimental data. The FSAC spontaneous and endothermic MB uptake at 30 °C gave high adsorption capacity of 184.40 mg/g. These results show that FSAC can be used as an efficient and low cost adsorbent for cationic dye removal.

© 2017 Elsevier B.V. All rights reserved.

## 1. Introduction

The exponential increase of pollutants in our environment due to society development through advancement in science and technology is becoming alarming. The environments usually polluted are water, land, and air, and pollution affects plants, animals, and other non-living things in the ecosystem. Polluted water (wastewater) contains several substances such as heavy metals, dyes, pesticides, pharmaceuticals, herbicides, among others depending on the source of the effluents [1].

Dye effluents are complex, highly visible, and undesirable due to their brilliance at low concentration. As such, their stable presence in waters is toxic and harmful to aquatic life as they impede sunlight penetration, thereby limiting the photosynthesis activities of the ecosystem [2]. Dye substances have high resistance to biodegradability and are stable in different weather conditions [3]. Stable dye substances affect the genetic mutation of reproducing animals; in addition, these stable dyes are major sources of cancer diseases; affect heartbeats; and cause jaundice, skin irritation, kidney, liver, and central nervous system dysfunction, and other numerous health challenges [4,5].

Many industries, including cosmetics, paper and pulp, electroplating, automobile, tanneries, and textiles, produce dye wastewater; thus, dye wastewater removal is one of the most significant environmental sustainable measures that are globally acknowledged [6]. To solve this problem, membrane, coagulation, advanced oxidation processes, electrochemical methods, and other technologies have been explored; however, various limitations inhibit their applicability [7]. The efficient, simple, and promising adsorption technology provide bail to purification of dye wastewater [8]. However, the expensive commercial activated carbon is the major challenge [9,10].

As search into sourcing renewable, cheap, environmentally friendly, and abundantly available precursor for production of adsorbents continues, activated carbons have been prepared from various cheap sources [11–15].

Daily consumption of various fish species has increased in numerous parts of the world. This results in generation of 50%–70% of original material in Fishermen's Market and handling industries [16]. In 2010 the total fish leftover in Malaysia only was around 1.77 million tons which costs about RM 6.8 million and among the total production >30% was solid waste consisting mainly of scale, bone, and skin [17]. Such waste is always hazardous which results in severe contamination of the environment by creating health issues and undesirable odor. Various agricultural wastes have been processed, activated and transformed into valuable materials to be used in various applications [18–24]. Therefore, fish waste management should be implemented and be a source of the production of high value-added products. In fact, fish scales mainly consist of protein (collagen) and hydroxyapatite (HAp) along with fatty acids, vitamins, antioxidant and trace elements [25,26]. Due to the presence of specific chemical groups such as hydroxyl, carboxyl, amine and amide, fish scales can be an alternative to commercial adsorbents because of their availability as wastes and being widely accessible [27].

* Corresponding author.
   E-mail address: chbassim@usm.my (B.H. Hameed).

The use of the adsorptive potentials of aquatic lives or fishery wastes (shrimps, crabs, and lobsters) [28] as an adsorbent for dye removal is now a research focus. Thus, the production of carbon-based adsorbent from fish scales is a promising way not only to generate low-cost adsorbent for water purification but also to re-purpose a rapidly accumulating disposal problem of industrial/municipal by-products [26].

In this work, feasibility of preparing high-surface-area nitrogen-rich mesoporous carbon material (FSAC) from fishery waste was investigated. The applicability of FSAC in treating dye effluents was tested by using the adsorbent to adsorb methylene blue (MB) dye from simulated wastewater. The adsorption equilibrium, kinetics and thermodynamics of the MB on FSAC were also studied.

## 2. Materials and methods

### 2.1. Chemicals and precursor

The adsorbate used was MB dye ($\lambda_{max} = 665$ nm, molecular weight = 373.9 g/mol, $C_{16}H_{14}N_3SCl. 3H_2O$,) procured from Sigma Aldrich (M), Malaysia, and was used without further purification. Appropriate quantity of MB was dissolved in double distilled water obtained from water treatment system USF ELGA to prepare stock solution. Working solution of desired concentration (25 mg/L–400 mg/L) was prepared by consecutive dilution of standard stock solution and used for entire study. Analytical grade sodium hydroxide and hydrochloric acid were supplied by Sigma Aldrich, Malaysia. Fish (*Labeo rohita*) scales were obtained from a local market in Penang, Malaysia.

### 2.2. Fish scales carbon material preparation

Dirt and gelatinous substances on the fish scales (FS) were removed by thorough washing with double distilled water fallowed by drying at 60 °C in an oven. The dried FS was carbonized by heating in a vertical tubular stainless steel reactor at 600 °C for 90 min in nitrogen (99.995%) flow (100 $cm^3$/min). The carbonized fish scale (CFS) was allowed to cool under $N_2$ gas flow and then ground and sieved into 0.4–0.5 mm particle sizes.

The resulting char was impregnated by NaOH at the ratio of 3:1 (NaOH:CFS) (wt:wt%) for 4 h fallowed by drying at 105 °C in an oven. The dried mixture was then activated by heating in a horizontal tubular stainless steel reactor at 800 °C for 90 min. in $N_2$ atmosphere (flow 100 $cm^3$/min). The sample was left to cool to room temperature under the same $N_2$ gas flow. After cooling, the FSAC was washed with HCl (1.0 mol/L) followed by hot distilled water until pH ~6.5. The FSAC was then kept for drying at 105 °C in an oven for 24 h and later on stored in closed voiles for future analysis.

### 2.3. Kinetics and equilibrium adsorption studies

MB adsorption onto the FSAC was carried out by batch experiments. 250 mL Erlenmeyer capped volumetric flasks were used for performing adsorption studies. In each flask, 200 mL of the required solution and fixed amount of the FSAC (0.2 g) were added. Solutions were continuously agitated at 125 rpm in isothermal water bath shaker for 24 h at desired temperature. At each predetermined time interval the MB final concentration was determined till the process attained equilibrium. UV/Visible Shimadzu, Model UV 1601, Japan, double beam spectrophotometer was employed to analyze the concentrations of MB by absorbance measurements at 665 nm.

To study the kinetics of MB adsorption by FSAC at different initial concentration (25, 50, 100, 150, 200, 300, and 400 mg/L), the Erlenmeyer flasks containing 200 mL each of the aqueous samples at their initial pH with 0.2 g FSAC added were placed in the shaker at 30 °C. At pre-set intervals of time, the residual MB concentration was determined and

the amount of the adsorbate adsorption, $Q_t$ (mg/g), at time t was evaluated as follows:

$$Q_t = \frac{(C_0 - C_t) W}{V} \tag{1}$$

where $C_0$ and $C_t$ are the initial and any time liquid-phase MB concentration, respectively; FSAC adsorbent mass is denoted by $M$ (g) and volume of MB solution by $V$ (L)

Adsorption equilibrium studies were repeated in a procedure similar to those of kinetic experiment. However, the MB dye concentration was measured at time t = 0 and equilibration time. Amount of adsorbed dye molecules at equilibration time per grams of FSAC solid was calculated as follows:

$$Q_e = \frac{(C_0 - C_e) W}{V} \tag{2}$$

where $C_e$ (mg/L) is the liquid-phase MB concentration at equilibration time (min). Kinetics and equilibrium adsorption studies were measured repeated at isothermal condition of 40 and 50 °C.

For studying the effect of pH on MB adsorption by FSAC, 100 mL of 100 mg/L adsorbate solution was measured and 0.1 M/1.0 M of both NaOH and HCl were used to adjust the solution to the desired pH. These samples were placed in the shaker set at 30 °C for equilibrium adsorption via batch experiments.

### 2.4. Characterization of FSAC adsorbent

Surface physical properties of FSAC were analyzed by Micromeritics (ASAP 2020, USA) using $N_2$ as adsorbate at − 196 °C. Micropore volume and surface area were obtained from surface area analysis technique by t-plot method. Scanning electron microscope (SEM) for FSAC was imaged using Zeiss Supra 35VP to obtain its morphology. Energy dispersive X-ray (EDAX) was employed for elemental analysis of the adsorbent using the same instrument with the SEM. The surface functional groups on adsorbent before and after adsorption were characterized by Perkin Elmer Spectrum GX Infrared Spectrometer with the wave number ranging from 400 to 4000 $cm^{-1}$ using potassium bromide disc sample method of investigation.

## 3. Results and discussion

### 3.1. FSAC characterization

Adsorption properties of activated carbons are invaluably affected by their porosity and surface area [29]. Enormous space is more available for adsorbate adsorbent contact on large surface area carbon materials than on a smaller surface. Aperture of the developed pore suggests whether adsorbate molecules can easily penetrate or not, whereas the amount or volume of the solute an adsorbent material can retain is determined by its pore volume [30]. The FSAC had a BET surface area of 1867.67 $m^2$/g, which is larger than surface sizes obtained by other researchers [31] and also comparable with some commercial activated carbon produced [32].

MB has the following molecular dimensions: 1.43 nm width, 0.40 nm thickness, and 0.61 nm depth [30]. The MB molecular size can easily penetrate the pore size and be retained in the pore volume of FSAC obtained as 2.5 nm and 0.38 $cm^3$/g, respectively. In accordance to the IUPAC classification of pore into micropore (<2 nm), mesopores (2–50 nm), and macropores (>50 nm), the FSAC pores were majorly mesopores [33]. The large surface area and porosity successfully developed on FSAC was attributed to the activation agent and temperature used, which are very influential activated carbon preparation process variables [34].

The $N_2$ adsorption–desorption isotherm plot on Fig. 1 revealed the presence of type 4 hysteresis loop at medium to high relative pressure
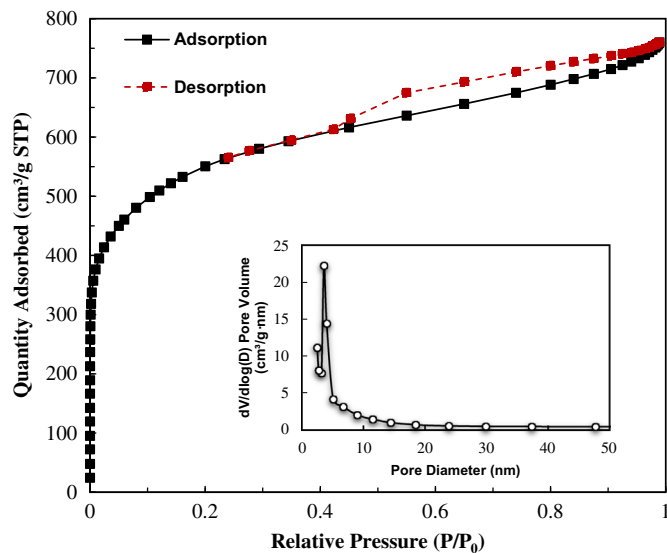
**Fig. 1.** Nitrogen adsorption-desorption isotherm plot for FSAC.



**Fig. 2.** (a) SEM for FSAC at 10,000× magnification; (b) elemental compositions and molar ratios of FSAC.

and a type IV isotherm, which on each layer adsorbed represents mono-layer capacity; such hysteresis loop is common in activated carbons [33]. This hysteresis loop is indicative of mesoporous adsorbent associated capillary condensation during adsorption–desorption [35].

The morphological structure of FSAC determined by SEM revealed some pores on the micrograph, as shown in the Fig. 2a. The EDX analysis (Fig. 2b) also revealed high (>70%) elemental composition of carbon and threshold content of heteroatoms (N: 19.45%; Ca: 0.02%). As per our previous study, the raw fish scales (FS) is composed by: C: 46.08%; N: 26.64%; O: 24.86%; Ca: 1.27%; P: 0.91%; S: 0.24%) [36]. The comparison between FSAC and FS revealed that the activation by NaOH resulted in the increase in carbon content accompanied by a slight decrease in the nitrogen content and the significant reduction of oxygen, calcium, phosphorus and sulfur due to the elimination of volatiles during activation process [37].

While considering the economic benefits, the production yield is always an important parameter. In this study, the yield of carbon material was calculated based on initial mass of CFS and was around 35%.

### 3.2. FSAC FTIR spectra

The FTIR spectra before and after adsorption of MB are presented in Fig. 3. Several functional group peaks were detected on the FSAC, and some were useful and involved in MB adsorption, whereas others were not as indicated by disappearance and shifting in wavenumber and unchanged wavenumbers (Fig. 3), respectively. Similar observation by other researchers has been reported [38]. The active functional groups on the FSAC that participated in binding the MB molecules were —OH, C—O, C═O, and —COO— representing respectively the hydroxyl, inorganic carbonates, cyclic acid anhydride, and carboxylic groups. The peak at 3420.90 cm$^{-1}$ on FSAC, which shifted to 3419.94 cm$^{-1}$, represents the O—H stretching vibration of the hydroxyl group [39]. The peaks on fresh FSAC at 1616.42, 1456.32, 1414.85, and 1032.85 cm$^{-1}$ attributed to asymmetric $CO_2$ stretch carboxylates; C═O groups (carbonyl anion), C—O stretch inorganic carbonates, primary alcohols, and phenols shifted to 1596.16, 1465, 1422.56, and 1033.89 cm$^{-1}$, respectively [30]. The wide stretch of O—H groups combined with stretches of C═O is diagnostic for carboxylic acids, which enhance MB adsorption on FSAC. Some N—H in-plane secondary amides and $NO_2$ scissors of nitro functional groups at wavenumbers of 1517 and 603.75 cm$^{-1}$, respectively, on FSAC surface remained stationary as they did not actively participated in the process of adsorption.

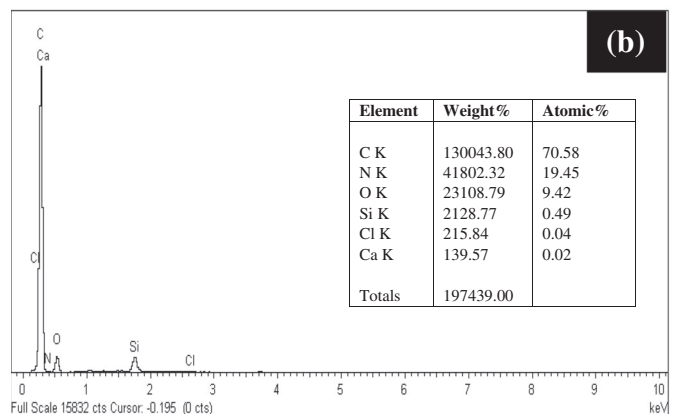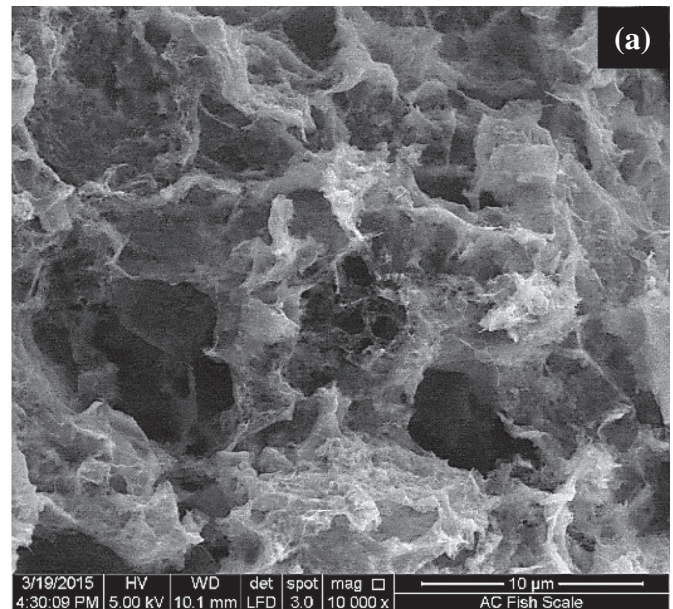### 3.3. Effect of MB initial concentrations

Concentration difference is a driving force in mass transfer operation. A range of 25–400 mg/L initial aqueous solution of MB was used to study its effect on MB adsorption by FSAC, and the profiles are
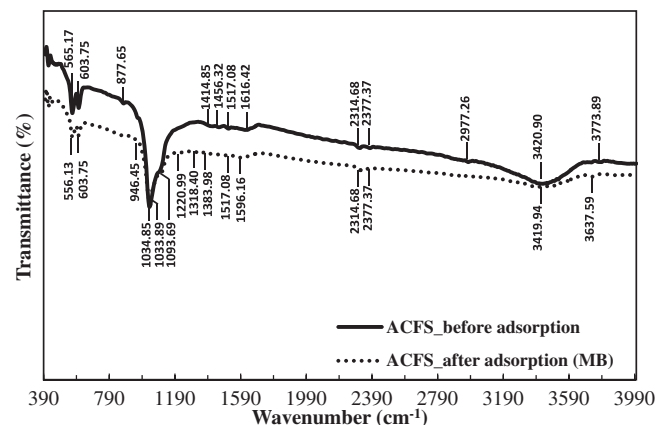


**Fig. 3.** FTIR spectra for FSAC (a) before adsorption (b) after adsorption.

presented in Fig. 4. The resistances between the adsorbent and aqueous phases were surmounted by driving force emanating from concentration difference such that larger adsorption was observed at higher initial solute concentration. However, higher percentage of MB adsorption and faster attainment of adsorption equilibrium were observed at lower initial solute concentration. This finding was attributed to spontaneous accessibility of the numerous vacant active sites on FSAC by the limited MB molecules in the lower initial sorbate concentration [2]. Longer time and lower percentage of adsorption at higher initial solute concentration were attributed to the saturation of the available active site present on FSAC and also to the less-available surface active sites on FSAC to preponderance MB solute ratio. Similar observation has been reported by other researchers [40]. Considering the initial solute concentrations (25, 50, 100, 150, 200, 300, 400 mg/L) studied, the equilibrium time was extended to 25 h.

### 3.4. Effect of variation of pH on MB adsorption onto FSAC

The surface chemistry of an adsorbent has invaluable influence on adsorption of adsorbate. This can be galvanized or stimulated by altering the initial pH, which can either impair or aggravate adsorbate adsorption. Investigation on the effects of pH variation on MB dye adsorption by FSAC was carried out in the pH range of 3–11. Profiles for the initial pH influence of MB adsorption are presented in Fig. 5. High initial pH values intensified both the adsorption capacity and the percentage removal of MB by FSAC. Acquisition of positive charges by the FSAC and protonation of $H^+$ ions at low pH concentrations may have competed with the positively charged MB molecules for the limited active sight on the adsorbent. At higher initial pH the enhanced adsorption may be explained by the involuntary compelling influence between the positive charged MB molecules and the negative charged FSAC surface. This observation is similar to reports of other researchers who equally attempted to investigate MB uptake through adsorption [38].

### 3.5. Adsorption isotherms

Equilibrium adsorption isotherm was studied to optimize the maximum adsorbent usage and to merge the most appropriate correlation
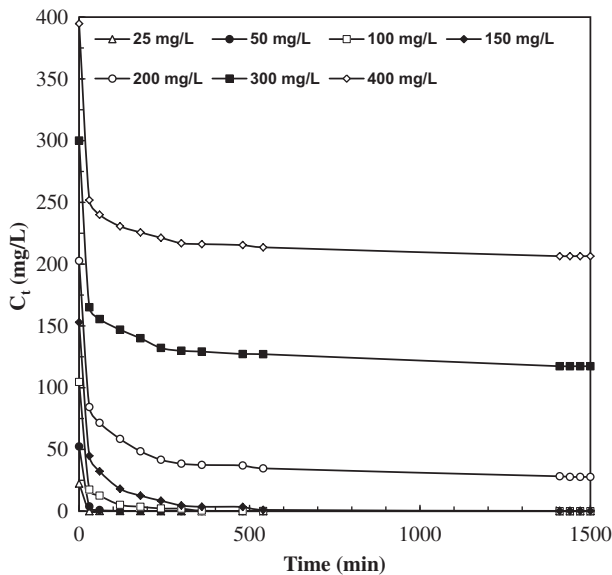


**Fig. 5.** Effect of pH on MB adsorption by FSAC (temperature = 30 °C, shaking speed = 125 rpm, adsorbent dose = 1 g/L).

that describes the distribution of adsorbate molecules between solid phase and liquid phase for MB adsorption plant design. Two of the most commonly used standard isotherms models, i.e., Langmuir and Freundlich isotherms, were evaluated. These two isotherm models are applied by researchers in either the non-linear or linearized forms, but due to the inconsistency of results or errors obtained after linearization [41], the non-linear form of the models was used in this study.

Langmuir equilibrium isotherm model [42] assumes adsorption to be monolayer type and describes the adsorbent surface as homogeneous having identical surface sites. The model equation can be expressed as

$$Q_e = \frac{Q_0 \times k_L \times C_e}{1 + k_L \times C_e} \tag{3}$$

where $K_L$ (L/mg) is constant of adsorption associated with free energy, $Q_0$ (mg/g) denotes the maximum adsorption capacities and $C_e$ (mg/L) denotes the equilibrium concentrations of MB.

Freundlich model [43] is the earliest sorption isotherm known. The model assumes that the energies on the sorption surface are heterogeneous, which varies due to surface coverage. The model equation can be expressed as

$$Q_e = k_F \times C_e^{1/n} \tag{4}$$



**Fig. 4.** Contact time and initial concentration effect on adsorption of MB on FSAC (temperature = 30 °C, shaking speed = 125 rpm, adsorbent dose = 1 g/L).
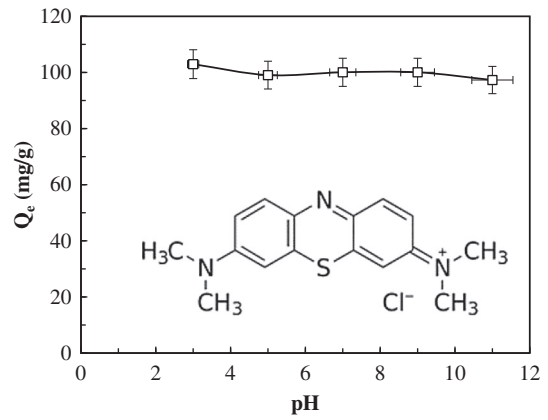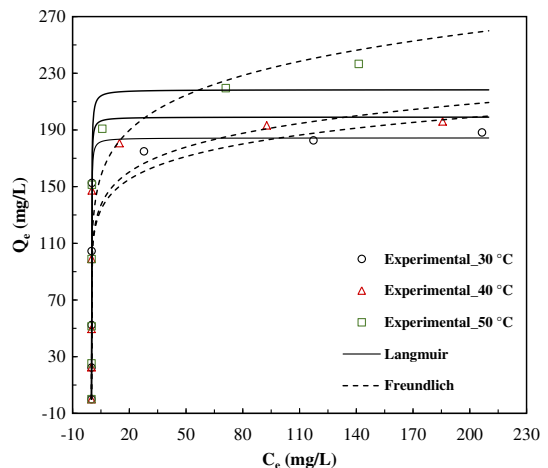


**Fig. 6.** Adsorption isotherm at different temperatures.

**Table 1**
Isotherm parameters of Freundlich and Langmuir models at various temperatures for MB adsorption on FSAC.

| Isotherms | Parameters | Temperature | | |
|-----------|-----------|-------|-------|-------|
| | | 30 °C | 40 °C | 50 °C |
| Langmuir | $Q_0$ | 184.40 | 199.10 | 214.40 |
| | $k_L$ | 13.220 | 14.000 | 16.420 |
| | $R^2$ | 0.946 | 0.943 | 0.972 |
| | RMSE | 16.534 | 17.796 | 12.778 |
| Freundlich | $k_F$ | 112.4 | 114.8 | 132.2 |
| | n | 9.295 | 8.525 | 7.867 |
| | $R^2$ | 0.811 | 0.811 | 0.902 |
| | RMSE | 30.993 | 30.701 | 9.551 |

where n and $k_F$ ($(mg/g)(L/mg)^{1/n}$) are Freundlich parameters in relation to the adsorption intensity and adsorption capacity, respectively. Simulation of the models revealed that both Langmuir and Freundlich expressions supported the FSAC adsorption data because of high $R^2$ values obtained from the models plots shown in Fig. 6. This can be adjudged by the sorption intensity on heterogeneous energies (112.4–132.2 mg/g) and monolayer coverage (184.40–214.40 mg/g), which had a corresponding $R^2$ range of 0.811–0.902 and 0.946–0.972 for Freundlich and Langmuir isotherm models, respectively (Table 1). Root mean square errors (RMSE) were calculated to evaluate the error of kinetic models and to draw a more reliable comparison that will justify the most fitted isotherm model. The $R^2$ and RMSE can be calculated according to the following expressions

$$R^2 = 1 - \frac{\sum_{n=1}^{n}\left(Q_{e.\ exp} - Q_{e.cal}\right)^2}{\sum_{n=1}^{n}\left(Q_{e.\ exp} - \overline{Q_{e.\ exp}}\right)^2} \tag{5}$$

$$RMSE = \sqrt{\frac{1}{n-1}\sum_{n=1}^{n}\left(Q_{e.\ exp} - Q_{e.cal}\right)^2} \tag{6}$$

Evaluation of the fitness of both models simulated data revealed lower values (≤17) of RMSE of Langmuir model when compared with Freundlich model, as presented in Table 1. This finding connotes that adsorption of MB by FSAC was limited to monolayer coverage, suggesting that each active site possesses regular and constant sorption capability. Increase in adsorption capacity of FSAC with temperature rise may have enhanced the kinetic energy of MB molecules onto the adsorbent surfaces from the bulk aqueous solution [29]. The adsorption capacity of FSAC for MB uptake obtained are comparable with other adsorbents [30,38,39,44] for similar pollutant removal from aqueous medium, as presented in Table 2.

### 3.6. Adsorption kinetics

For practical designing of an adsorption system it is essential to have knowledge about potential controlling steps and the mechanism of adsorption, which is provided by adsorption kinetics. Adsorption rate of MB molecules onto FSAC was modeled using pseudo- first-order (PFO) and pseudo-second-order (PSO) kinetic equations. PFO kinetics assumes that the amount of adsorbate adsorbed is proportional to the initial sorbate concentration and adsorbent dosage, which is entirely a physisorption process [30]. PSO kinetics has the base on the premises that chemisorption is the model's rate-limiting step, which involves electron exchange between adsorbate and adsorbent [45].

The non-linear PFO model [46] equation is as

$$Q_t = Q_e \times \left(1 - e^{-k_1 t}\right) \tag{7}$$

where $k_1$ is the PFO rate constant and t is the contact time in min.

The non-linear PSO model [45] is given as

$$Q_t = \frac{k_2 Q_e^2 t}{1 + k_2 Q_e t} \tag{8}$$

where $k_2$ (g/mg/min) is the constant known as velocity or rate constant for second order kinetics.

The model parameters presented in Table 3 were obtained from the plots ($Q_t$ against t) of the two kinetic equations shown in Fig. 7. Simulation of the two kinetic models revealed appreciable hike in adsorption capacity when initial MB concentration was increased. This observation was attributed to the increase in frequency of MB molecule interaction with FSAC surface at higher initial concentration, which also corresponds to high driving force mass transfer of the process [38]. The preponderance of MB molecules at higher initial concentration also shortened the time taken for the molecules to access the active surface of the FSAC.

The calculated $Q_e$ values of the two models agreed with the experimentally obtained data as adjudged by the high $R^2$ values (>0.957). However, the $R^2$ of PSO kinetics was slightly higher. The RMSE presented in Table 3 showed an error interval of 0.052–9.464 and 0.278–4.991 for PFO and PSO kinetic models, respectively. The lower error values recorded for PSO kinetic connotes that it was the best model that described adsorption of MB by FSAC.

Therefore, chemisorption (involving chemical reactions) characterized MB adsorption by FSAC. This finding further confirmed the monolayer coverage of MB on FSAC adjudged by Langmuir as the best fitted isotherm and that any additional layers that followed may be physically adsorbed MB molecules [40,47]. This observation is similar to reports by other researchers.

### 3.7. Thermodynamic modeling

Adsorption thermodynamic parameters; the Gibbs free energy ($\Delta G^0$), enthalpy ($\Delta H^0$), and entropy ($\Delta S^0$) can reveal the mechanism

**Table 2**
Adsorption capacity comparisons of adsorbents for methylene blue.

| Adsorbent | Maximum monolayer adsorption capacity $Q_0$ (mg/g) | Temperature (°C) | Reference |
|-----------|---------------------------------------------------|------------------|-----------|
| Anaerobic digestion residue | 9.5 | 40 | [30] |
| Palm bark | 2.66 | 40 | [30] |
| Eucalyptus | 2.06 | 40 | [30] |
| Pineapple stem | 119 | 30 | [38] |
| Activated rice husk treated with phosphoric acid | 578 | 30 | [39] |
| Bone char | 160 | 25 | [44] |
| Fish scale activated material | 184.40 | 30 | This work |

**Table 3**
Adsorption kinetic parameters for MB onto FSAC on 30 °C at various initial concentrations.

| MB concentration (mg/L) | $Q_{e,exp}$ | Pseudo-first-order | | | | Pseudo-second-order | | | |
|---|---|---|---|---|---|---|---|---|---|
| | | $Q_{e,cal}$ | $k_1$ | $R^2$ | RMSE | $Q_{e,cal}$ | $k_2$ | $R^2$ | RMSE |
| 25 | 22.33 | 22.29 | 0.380 | 0.999 | 0.052 | 22.31 | 0.516 | 0.999 | 0.498 |
| 50 | 52.35 | 52.25 | 0.087 | 0.999 | 0.169 | 52.63 | 8.66E−03 | 0.999 | 0.278 |
| 100 | 104.55 | 102.90 | 0.057 | 0.990 | 2.634 | 105.20 | 140E−03 | 0.999 | 0.848 |
| 150 | 152.62 | 148.00 | 0.037 | 0.976 | 6.044 | 153.90 | 4.54E−04 | 0.998 | 1.869 |
| 200 | 174.90 | 165.70 | 0.034 | 0.958 | 9.094 | 173.70 | 3.34E−04 | 0.993 | 3.801 |
| 300 | 182.65 | 172.00 | 0.043 | 0.957 | 9.464 | 179.00 | 4.44E−04 | 0.988 | 4.991 |
| 400 | 188.25 | 179.10 | 0.047 | 0.960 | 8.139 | 185.30 | 5.02E−04 | 0.993 | 3.926 |

and adsorption behavior at different temperatures. The values of these thermodynamic parameters ($\Delta G^0$, $\Delta H^0$, and $\Delta S^0$) at 30, 40 and 50 °C can be obtained as follows:

$$\Delta G^\circ = -R\,T\,\ln K_0 \tag{9}$$

$$\ln K_d = \frac{\Delta S^\circ}{R} - \frac{\Delta H^\circ}{RT} \tag{10}$$

where $R$ (8.314 J/mol.K) is the universal gas constant, $T$ (K) is the absolute solution temperature, and $K_0$ provides the adsorption distribution coefficient. The values of $\Delta H^0$ and $\Delta S^0$ are calculated from the $\ln K_0$ vs $1/T$ plot which gives a straight line with a slope and intercept of $\Delta H^0/R$ and $\Delta S^0/R$, respectively.

The negative $\Delta G^0$ values ($-4637.69$, $-6511.45$, $-9428.57$ J/mol) confirmed the spontaneous nature of the adsorption. Also the $\Delta G^0$ values decreased with increase in temperature which demonstrated that the adsorption process was favorable at high temperatures [36]. On the other hand, the positive $\Delta H^0$ value (67.77 kJ/mol) further revealed the endothermic nature of the adsorption process. Moreover, the value of $\Delta S^0$ was 238.44 J/mol·K, which indicated increased randomness at the solid–solution interface with the loading of MB molecules onto the external and internal surfaces of the FSAC.
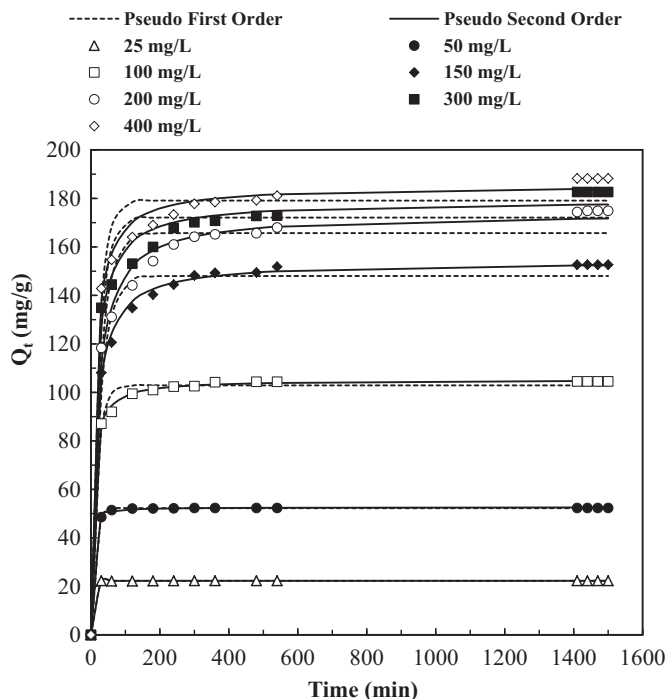


**Fig. 7.** PFO and PSO kinetic fittings for FSAC adsorption FSAC at 30 °C.

## 4. Conclusion

The feasibility of producing mesoporous and high surface area nitrogen-rich carbon material (FSAC) from fishery waste was substantiated. FSAC exhibited high surface area (1867 m²/g) and mesoporosity (2.5 nm). The adsorption results showed that Langmuir isotherm and PSO adsorption models adequately described the experimentally obtained data. The values of the heat adsorption at various temperatures indicate that the system FSAC–MB interaction were chemical. The adsorbent FSAC demonstrated effectiveness in removing cationic dyes with high MB adsorption capacity of 184.40 mg/g at 30 °C. Therefore, FSAC can be used as a cleaner bio-material adsorbent and an alternative to many commercial and others agricultural byproducts-based carbonaceous adsorbents for the uptake of organic pollutants from aqueous solution.

## References

[1] M. Kayhanian, B.D. Fruchtman, J.S. Gulliver, C. Montanaro, E. Ranieri, S. Wuertz, Review of highway runoff characteristics: comparative analysis and universal implications, Water Res. 46 (2012) 6609–6624.
[2] M.S. Sajab, C.H. Chia, S. Zakaria, P.S. Khiew, Cationic and anionic modifications of oil palm empty fruit bunch fibers for the removal of dyes from aqueous solutions, Bioresour. Technol. 128 (2013) 571–577.
[3] Z. Carmen, S. Daniela, Textile organic dyes–characteristics, polluting effects and separation/elimination procedures from industrial effluents–a critical overview, Org. Pollut. Ten Years After Stock. Conv. Anal. Updat 2012, pp. 55–81.
[4] E. Alver, A.Ü. Metin, Anionic dye removal from aqueous solutions using modified zeolite: adsorption kinetics and isotherm studies, Chem. Eng. J. 200 (2012) 59–67.
[5] M.A.M. Salleh, D.K. Mahmoud, W.A.W.A. Karim, A. Idris, Cationic and anionic dye adsorption by agricultural solid wastes: a comprehensive review, Desalination 280 (2011) 1–13.
[6] N.F. Ali, R.S.R. El-Mohamedy, Microbial decolourization of textile waste water, J. Saudi Chem. Soc. 16 (2012) 117–123.
[7] V.K. Gupta, Application of low-cost adsorbents for dye removal–a review, J. Environ. Manag. 90 (2009) 2313–2342.
[8] W.A. Khanday, F. Marrakchi, M. Asif, B.H. Hameed, Mesoporous zeolite–activated carbon composite from oil palm ash as an effective adsorbent for methylene blue, J. Taiwan Inst. Chem. Eng. 70 (2017) 32–41.
[9] P. Nowicki, R. Pietrzak, Carbonaceous adsorbents prepared by physical activation of pine sawdust and their application for removal of NO₂ in dry and wet conditions, Bioresour. Technol. 101 (2010) 5802–5807.
[10] J. Kaźmierczak, P. Nowicki, R. Pietrzak, Sorption properties of activated carbons obtained from corn cobs by chemical and physical activation, Adsorption 19 (2013) 273–281.
[11] A.A. Ahmad, B.H. Hameed, A.L. Ahmad, Removal of disperse dye from aqueous solution using waste-derived activated carbon: optimization study, J. Hazard. Mater. 170 (2009) 612–619.
[12] K.Y. Foo, B.H. Hameed, Factors affecting the carbon yield and adsorption capability of the mangosteen peel activated carbon prepared by microwave assisted K₂CO₃ activation, Chem. Eng. J. 180 (2012) 66–74.
[13] K.Y. Foo, B.H. Hameed, Preparation and characterization of activated carbon from pistachio nut shells via microwave-induced chemical activation, Biomass Bioenergy 35 (2011) 3257–3261.
[14] M.A. Islam, M.J. Ahmed, W.A. Khanday, M. Asif, B.H. Hameed, Mesoporous activated carbon prepared from NaOH activation of rattan (*Lacosperma secundiflorum*) hydrochar for methylene blue removal, Ecotoxicol. Environ. Saf. 138 (2017) 279–285.
[15] M. Danish, W.A. Khanday, R. Hashim, N.S.B. Sulaiman, M.N. Akhtar, M. Nizami, Application of optimized large surface area date stone (*Phoenix dactylifera*) activated carbon for rhodamin B removal from aqueous solution: Box-Behnken design approach, Ecotoxicol. Environ. Saf. 139 (2017) 280–290.
[16] G.K. Kafle, S.H. Kim, K.I. Sung, Ensiling of fish industry waste for biogas production: a lab scale evaluation of biochemical methane potential (BMP) and kinetics, Bioresour. Technol. 127 (2013) 326–336.

[17] S.A. Rahman, H. Zambry, S. Basha, S. Kamarzaman, A.J.K. Chowdhury, The potential role of Red Tilapia (*Oreochromis niloticus*) scales: allergic reaction test in mice, J. Appl. Pharm. Sci. 3 (2013) 45.

[18] G. Tzvetkov, S. Mihaylova, K. Stoitchkova, P. Tzvetkov, T. Spassov, Mechanochemical and chemical activation of lignocellulosic material to prepare powdered activated carbons for adsorption applications, Powder Technol. 299 (2016) 41–50.

[19] P. Nowicki, J. Kazmierczak, R. Pietrzak, Comparison of physicochemical and sorption properties of activated carbons prepared by physical and chemical activation of cherry stones, Powder Technol. 269 (2015) 312–319.

[20] Z. Guo, A. Zhang, J. Zhang, H. Liu, Y. Kang, C. Zhang, An ammoniation-activation method to prepare activated carbon with enhanced porosity and functionality, Powder Technol. (2016).

[21] Y. Li, Y. Li, L. Li, X. Shi, Z. Wang, Preparation and analysis of activated carbon from sewage sludge and corn stalk, Adv. Powder Technol. 27 (2016) 684–691.

[22] J. Kazmierczak-Razna, P. Nowicki, R. Pietrzak, The use of microwave radiation for obtaining activated carbons enriched in nitrogen, Powder Technol. 273 (2015) 71–75.

[23] M. Ghasemi, M.Z. Khosroshahy, A.B. Abbasabadi, N. Ghasemi, H. Javadian, M. Fattahi, Microwave-assisted functionalization of *Rosa canina*-L fruits activated carbon with tetraethylenepentamine and its adsorption behavior toward Ni (II) in aqueous solution: kinetic, equilibrium and thermodynamic studies, Powder Technol. 274 (2015) 362–371.

[24] W.A. Khanday, G. Kabir, B.H. Hameed, Catalytic pyrolysis of oil palm mesocarp fibre on a zeolite derived from low-cost oil palm ash, Energy Convers. Manag. 127 (2016) 265–272.

[25] N. Muhammad, G. Gonfa, A. Rahim, P. Ahmad, F. Iqbal, F. Sharif, et al., Investigation of ionic liquids as a pretreatment solvent for extraction of collagen biopolymer from waste fish scales using COSMO-RS and experiment, J. Mol. Liq. 232 (2017) 258–264.

[26] L. Nielsen, P. Zhang, T.J. Bandosz, Adsorption of carbamazepine on sludge/fish waste derived adsorbents: effect of surface chemistry and texture, Chem. Eng. J. 267 (2015) 170–181.

[27] J.A. Mota, R.A. Chagas, E.F.S. Vieira, A.R. Cestari, Synthesis and characterization of a novel fish scale-immobilized chitosan adsorbent—preliminary features of dichloro-phenol sorption by solution calorimetry, J. Hazard. Mater. 229–230 (2012) 346–353.

[28] G. Crini, P.-M. Badot, Application of chitosan, a natural aminopolysaccharide, for dye removal from aqueous solutions by adsorption processes using batch studies: a review of recent literature, Prog. Polym. Sci. 33 (2008) 399–447.

[29] D. Angin, Utilization of activated carbon produced from fruit juice industry solid waste for the adsorption of Yellow 18 from aqueous solutions, Bioresour. Technol. 168 (2014) 259–266.

[30] L. Sun, S. Wan, W. Luo, Biochars prepared from anaerobic digestion residue, palm bark, and eucalyptus for adsorption of cationic methylene blue dye: characterization, equilibrium, and kinetic studies, Bioresour. Technol. 140 (2013) 406–413.

[31] H. Demiral, İ. Demiral, F. Tümsek, B. Karabacakoğlu, Adsorption of chromium(VI) from aqueous solution by activated carbon derived from olive bagasse and applicability of different adsorption models, Chem. Eng. J. 144 (2008) 188–196.

[32] D.M. Ginosar, L.M. Petkovic, K.C. Burch, Commercial activated carbon for the catalytic production of hydrogen via the sulfur–iodine thermochemical water splitting cycle, Int. J. Hydrog. Energy 36 (2011) 8908–8914.

[33] K.S. Sing, Reporting physisorption data for gas/solid systems with special reference to the determination of surface area and porosity (recommendations 1984), Pure Appl. Chem. 57 (1985) 603–619.

[34] O. Pezoti, A.L. Cazetta, K.C. Bedin, L.S. Souza, A.C. Martins, T.L. Silva, et al., NaOH-activated carbon of high surface area produced from guava seeds as a high-efficiency adsorbent for amoxicillin removal: kinetic, isotherm and thermodynamic studies, Chem. Eng. J. 288 (2016) 778–788.

[35] Y.-M. Chang, W.-T. Tsai, M.-H. Li, Characterization of activated carbon prepared from chlorella-based algal residue, Bioresour. Technol. 184 (2015) 344–348.

[36] F. Marrakchi, M.J. Ahmed, W.A. Khanday, M. Asif, B.H. Hameed, Mesoporous carbonaceous material from fish scales as low-cost adsorbent for reactive orange 16 adsorption, J. Taiwan Inst. Chem. Eng. 71 (2017) 47–54.

[37] P. Nowicki, R. Pietrzak, H. Wachowska, Comparison of physicochemical properties of nitrogen-enriched activated carbons prepared by physical and chemical activation of brown coal, Energy Fuel 22 (2008) 4133–4138.

[38] B.H. Hameed, R.R. Krishni, S.A. Sata, A novel agricultural waste adsorbent for the removal of cationic dye from aqueous solutions, J. Hazard. Mater. 162 (2009) 305–311.

[39] Y. Chen, S.-R. Zhai, N. Liu, Y. Song, Q.-D. An, X.-W. Song, Dye removal of activated carbons prepared from NaOH-pretreated rice husks by low-temperature solution-processed carbonization and H$_3$PO$_4$ activation, Bioresour. Technol. 144 (2013) 401–409.

[40] H.-C. Tao, H.-R. Zhang, J.-B. Li, W.-Y. Ding, Biomass based activated carbon obtained from sludge and sugarcane bagasse for removing lead ion from wastewater, Bioresour. Technol. 192 (2015) 611–617.

[41] Y.-S. Ho, Selection of optimum sorption isotherm, Carbon N. Y. 42 (2004) 2115–2116.

[42] I. Langmuir, The constitution and fundamental properties of solids and liquids. Part I. Solids, J. Am. Chem. Soc. 38 (1916) 2221–2295.

[43] H.M.F. Freundlich, Over the Adsorption in Solution, 57, 1906.

[44] A.W.M. Ip, J.P. Barford, G. McKay, A comparative study on the kinetics and mechanisms of removal of Reactive Black 5 by adsorption onto activated carbons and bone char, Chem. Eng. J. 157 (2010) 434–442.

[45] Y.S. Ho, G. McKay, Pseudo-second order model for sorption processes, Process Biochem. 34 (1999) 451–465.

[46] S. Lagergren, About the Theory of So-called Adsorption of Soluble Substances, 1898.

[47] E.N. El Qada, S.J. Allen, G.M. Walker, Adsorption of methylene blue onto activated carbon produced from steam activated bituminous coal: a study of equilibrium adsorption isotherm, Chem. Eng. J. 124 (2006) 103–110.